

Supplementary Material

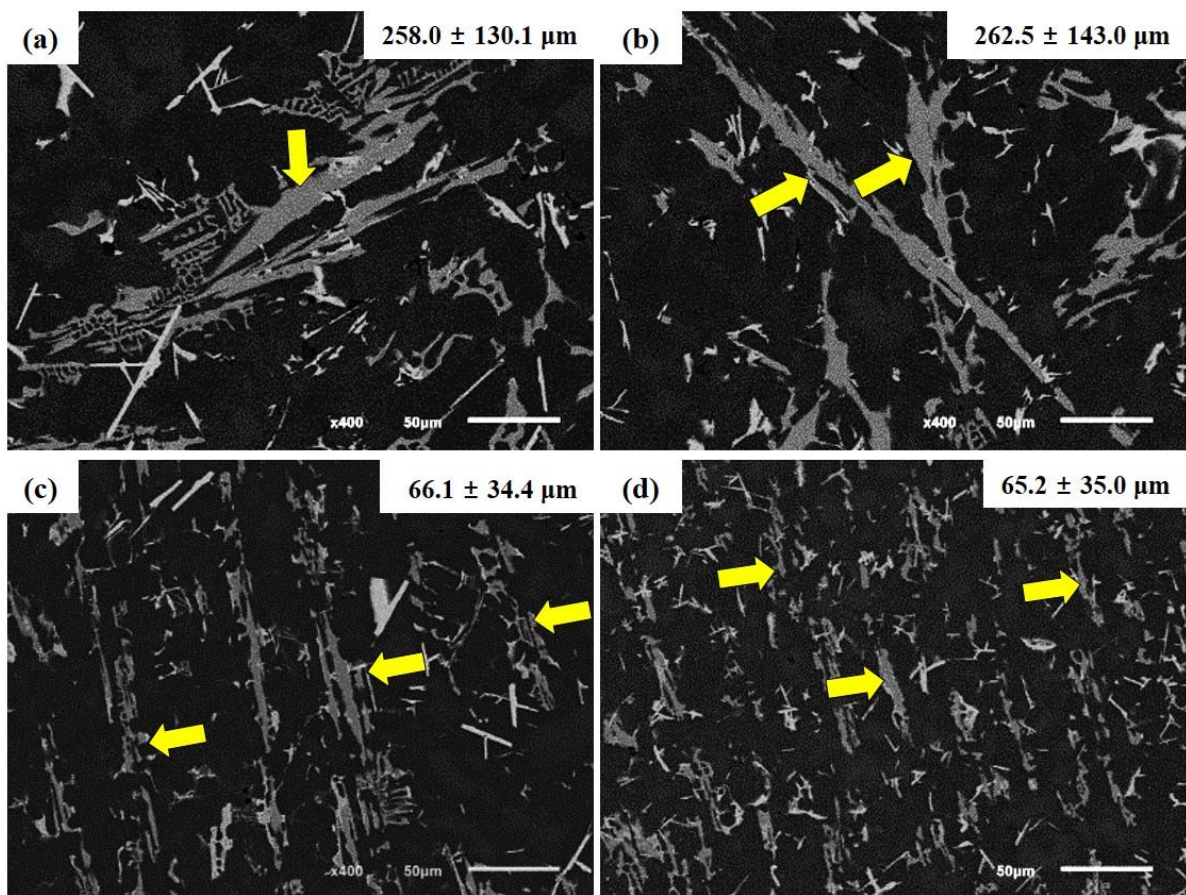
Hierarchical refinement of primary phases in a multicomponent Al-14Si-CuNiMg casting alloy by ultrasonic melt treatment

Authors: Min-Su Jo^{1,2}, Young-Hee Cho^{*,1}, Jung-Moo Lee¹, Soo-Bae Kim¹, Jun-Yun Kang¹, Jae-Gil Jung¹, and Jae-il Jang²

1. Division of Metallic Materials, Korea Institute of Materials Science, Changwon 51508, Korea

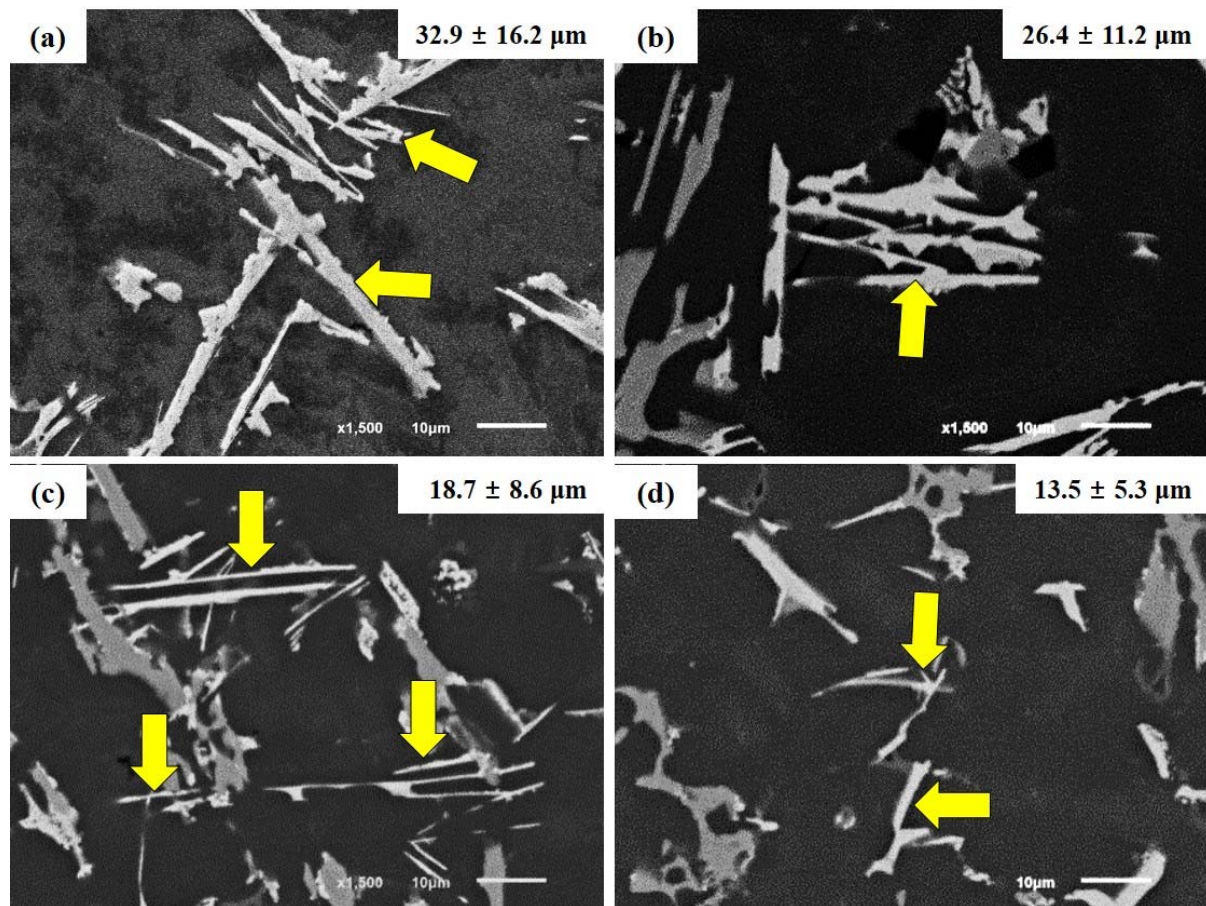
2. Division of Materials Science and Engineering, Hanyang University, Seoul 04763, Korea

*Corresponding author: y.cho@kims.re.kr



Supplementary Figure S1. BSE images showing Al_9FeNi intermetallic phases formed in the T7 treated alloys solidified at cooling rates of (a, b) 4 K/sec and (c, d) 32 K/sec: (a, c) without UST and (b, d) with UST. The average length of Al_9FeNi is also indicated in the inset of each image.

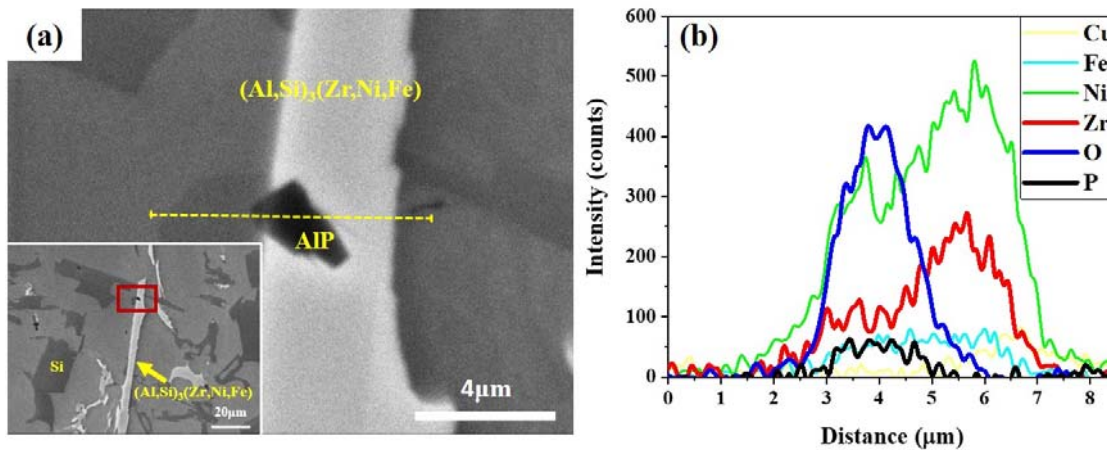
Supplementary Figure S1 exhibits BSE images showing Al_9FeNi phases (arrowed) formed in the T7 treated alloys. The average size with standard deviation is also indicated in the inset of each figure. Figs. S1(a, b) and S1(c, d) show the Al_9FeNi phases in the alloys solidified at the cooling rate of 4 and 32 K/s, respectively while Figs. S1(a, c) and S1(b, d) shows Al_9FeNi phases in the alloys without UST and with UST, respectively. The Al_9FeNi phases in both the alloys with and without UST, exhibit a fishbone morphology with the average length of approximately 260 and 65 μm at 4 and 32K/s, respectively. It should be noted that UST is unlikely to refine the Al_9FeNi phases while fast cooling rate has a certain effect on the structural refinement.



Supplementary Figure S2. BSE images showing $\text{Al}_3(\text{Cu},\text{Ni})_2$ intermetallic phases formed in the T7 treated alloys solidified at cooling rates of (a, b) 4 K/sec and (c, d) 32 K/sec: (a,

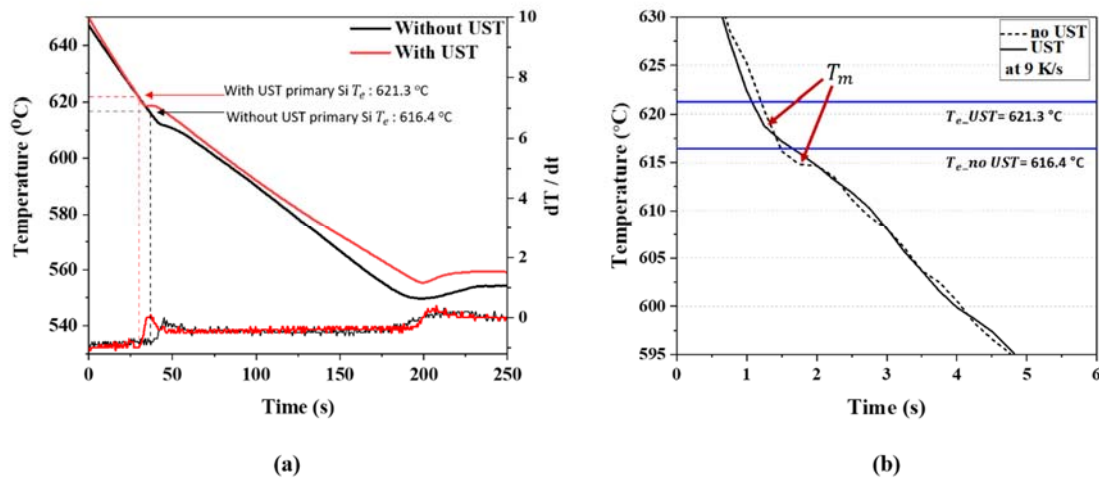
c) without UST and (b, d) with UST. The max. length of $\text{Al}_3(\text{Cu,Ni})_2$ is also indicated in the inset of each image.

Supplementary Figure S2 that the BES image showing $\text{Al}_3(\text{Cu,Ni})_2$ phases (arrowed) formed in the T7 treated alloys with and without UST solidified at cooling rates of 4 and 32 K/s. The order of each image arrangement in Fig. S2 is the same as Fig. S1. It is typically observed that the $\text{Al}_3(\text{Cu,Ni})_2$ phase has a needle-like shape with the maximum size of a few tens of μm . The average size with standard deviation was determined by image analysis and the results are indicated in the inset of each image. It was found that UST slightly refined the average size of the $\text{Al}_3(\text{Cu,Ni})_2$ phases from 33 to 26 μm at 4 K/s. The ultrasonic refinement becomes more pronounced at 32 K/s, significantly reducing the average size to 14 μm .



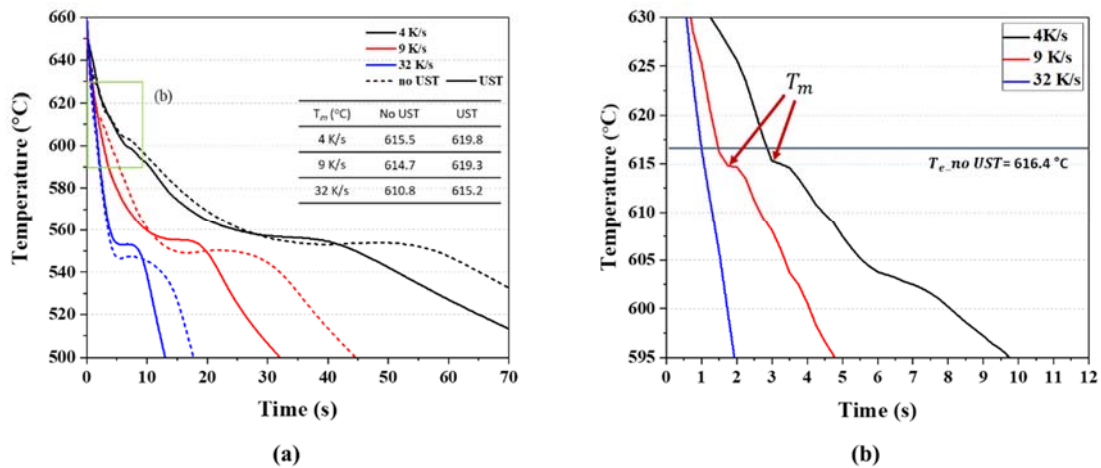
Supplementary Figure S3. SEM-EDS line-scan analysis across an $(\text{Al,Si})_3(\text{Zr,Ni,Fe})$ phase containing an AIP particle in the T7 treated alloy without UST solidified at 4K/s: (a) SEM image showing the line scan position (dashed line) across the $(\text{Al,Si})_3(\text{Zr,Ni,Fe})$ and the AIP phases and (b) the corresponding EDS line scan results illustrating the distribution of elements present in the phases.

Supplementary Fig. S3(a) shows a SEM image exhibiting an $(\text{Al,Si})_3(\text{Zr,Ni,Fe})$ phase containing an internal particle in the T7 treated alloy without UST solidified at 4 K/s. Inset image of Fig. S3(a) shows the overall image field involving the area of interest. As shown in Fig. S3(b), the distribution of P and O corresponds well with the internal particle while the surrounding phase consists of Ni, Fe and Zr. More importantly, the EDS line-scan analysis across the yellow dotted line in Fig. S3(a) confirms that the internal particle is P-rich phase, most probably AIP phase. This result has been further confirmed by our recent study [8] revealing that AIP can nucleate $(\text{Al,Si})_3(\text{Zr,Ni,Fe})$ intermetallics.



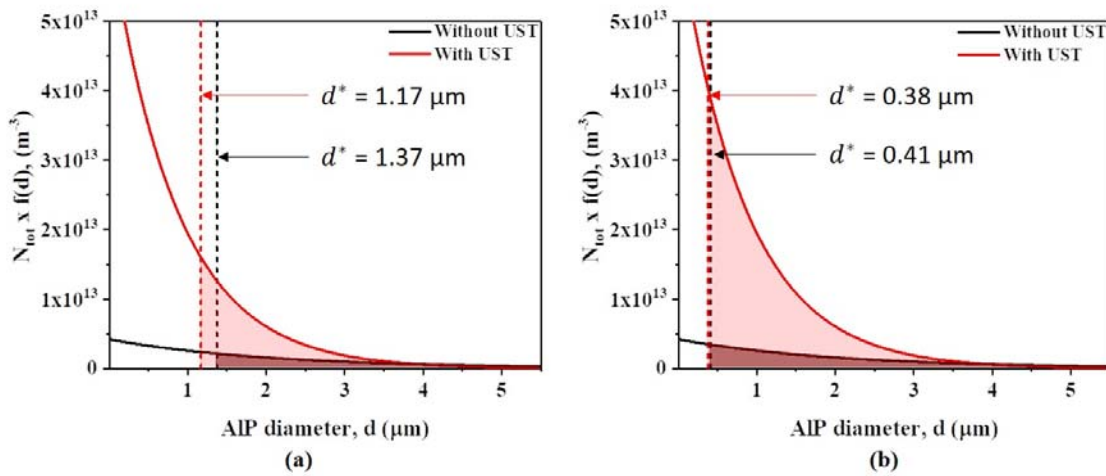
Supplementary Figure S4. (a) Cooling curves achieved during the solidification of the alloys with and without UST solidified at a cooling rate of ~ 0.8 K/s showing the reaction of primary Si at the temperature range of 610-620 °C (b) Enlarged cooling curves of the alloys with and without UST, solidified at 9 K/s, showing the T_m observed prior to the recalescence.

Supplementary Figure S4(a) shows cooling curves of the Al-14Si alloys with and without UST, experimentally achieved during the solidification at a cooling rate of ~ 0.8 K/s. Fig. S4(b) shows enlarged cooling curves of the alloys with and without UST, solidified at 9 K/s, showing the T_m prior to the recalescence. The cooling curves were measured at the slow cooling in order to precisely determine the solidification starting temperature (T_e). The maximum undercooling for nucleation ($\Delta T_m = T_e - T_m$) was then determined with the accurate detection of T_m (i.e. the minimum temperature prior to recalescence) from the cooling curves achieved at different cooling rates of 4, 9 and 32 K/s. The T_e of primary Si was determined by the intersection of the tangent of the derivative temperature curves in Fig. S4. The T_e values of primary Si formed in the alloys with and without UST are 621.3 °C and 616.4 °C, respectively, indicating that UST significantly increased the nucleation temperature of primary Si.



Supplementary Figure S5. (a) Cooling curves achieved during the solidification of the alloys with and without UST solidified at various cooling rates of 4, 9, 32 K/s. (b) Enlarged cooling curves showing the primary Si reaction of the alloys without UST, the most notably detected in the early stage of solidification.

Supplementary Figure S5(a) shows cooling curves of the Al-14Si alloys with and without UST, experimentally achieved during the solidification at a cooling rates of 4, 9 and 32 K/s. The maximum undercooling for nucleation ($\Delta T_m = T_e - T_m$) was then determined with the accurate detection of T_m (i.e. the minimum temperature prior to recalescence) from cooling curves achieved at different cooling rates of 4, 9 and 32 K/s. Fig. 5(b) shows enlarged cooling curves showing the primary Si reaction of the alloys without UST. Enlarged cooling curves at without UST showing the primary Si reaction the most notably detected in the early stage of solidification. The T_m values were analyzed as 615.5, 614.7 and 610.8 °C for the alloy without UST and 619.8, 619.3 and 615.2 °C for the alloy with UST at cooling rates of 4, 9 and 32 K/s, respectively.



Supplementary Figure S6. Distribution of the total numbers of AIP nucleants present in the alloys with and without UST as a function of the diameter. The shaded areas under the curve indicate the total number of AIP activated to nucleate the primary phases in the alloys with and without UST, solidified at a cooling rates of (a) 9 K/s and (b) 32 K/s.

Supplementary Figure S6 exhibits the distribution of the total numbers of AIP nucleant particles in the alloys with and without UST. As previously explained, the experimentally determined ΔT_m at the cooling rates of 9 and 32 K/s yields the different values of the critical diameter of the nucleant particle, d^* (see also Eq. 2 in the manuscript). This enables us to predict the total number of AIP activated to nucleate the primary phases at each cooling rate by analysing the shaded areas under curve as indicated in Fig. S6. It was found that ΔT_m increases with increase in the cooling rate while d^* inversely decreases. Eventually, the number of activated nucleation sites increases as the cooling rate increases and thus the refining efficiency increases.